PROGRESS
IN COLOR, COLORANTS AND COATINGS

available online @ www.pccc.icrc.ac.ir

Ministry of Science, Research and Technology
Institute for Color Science and Technology

Progress in Color Colorants Coating 15 (2022), 285-293

3-Nitrobenzaldehyde-4-phenylthiosemicarbazone as Active Corrosion Inhibitor for Mild Steel in a Hydrochloric Acid Environment

A. M. Mustafa[1], Z. S. Abdullahe[1], F. F. Sayyid[2], M. M. Hanoon[1], A. A. Alamiery[3, 4*], W.N.R.W. Isahak[3]

[1.] Production Engineering and Metallurgy, University of Technology-Iraq, P.O. Box: 10001, Baghdad, Iraq.
[2.] Chemistry Department, Al-Mustansiriyah University, P.O. Box: 10001, Baghdad, Iraq.
[3.] Energy and Renewable Energies Technology Center, Technology- Iraq, P.O. Box: 10001, Baghdad, Iraq.
[4.] Department of Chemical and Process Engineering, Faculty of Engineering and Built Environment, University Kebangsaan Malaysia, 43600 UKM Bangi, Selangor, Malaysia

ARTICLE INFO

Article history:
Received: 24 July 2021
Final Revised: 10 Dec 2021
Accepted: 12 Dec 2021
Available online: 12 Apr 2022

Keywords:
Thiosemicarbazone
Langmuir
Inhibition efficiency
Corrosion inhibitor
HCl

ABSTRACT

Natural and synthetic organic compounds were used as corrosion inhibitors to produce coordination complexes with metallic surface utilizing the active sites. These metallic complexes occupy a significant surface area on the metallic surface, therefore coating the metallic surface and shielding the metallic surface from acidic solutions. In the current study, a new Schiff base, namely (3-nitrobenzaldehyde)-4-phenylthiosemicarbazone (3N-4P), was designed and synthesized. The chemical structure of 3N-4P was determined using spectroscopic methods such as infrared (IR) and proton and carbon-13 nuclear magnetic resonance (^{1}H and ^{13}C-NMR) and CHN-analysis. The corrosive inhibitory potential of the 3N-4P was tested on mild steel (MS) coupons in a 1 M HCl utilizing weight loss techniques. The inhibitive efficiency (IE%) of 3N-4P increased with 3N-4P concentration increases and decreased with increasing temperature. The experimental findings revealed that 3N-4P molecules obeyed the Langmuir adsorption isotherm. Scanning by electron microscope (SEM) technology measured the uninhibited and inhibited coupon surface. Prog. Color Colorants Coat. 15 (2022), 285-293© Institute for Color Science and Technology.

1. Introduction

Chemical purification, descaling, and pickling of various alloying compositions and materials were performed in acidic environments. [1-7]. Metallurgical analysis is a basic technical level for removing metal oxides created during the annealing process [8-10]. Corrosion was always one of the fundamental problems of metallic structures since the economic costs resulting from corrosion failure are relatively high. Furthermore, corrosion failure poses a public risk; therefore, it is necessary to develop new materials which will retard corrosion on metallic structures, particularly in acidic environments. The organic complexes, particularly those with a heteroatom, like O, S, N, and P, were often utilized as corrosion inhibitors to mitigate the corrosions due to their ease of use, effectiveness, and economic aspects. In addition, the existence of the heteroatoms plays the role of an active center adsorbing over the metallic surfaces and mitigating the metallic corrosion [11-22]. Corresponding to other reported technologies on corrosion protection, utilizing corrosion inhibitors is

*Corresponding author: *100173@uotednology.edu.iq
dr.ahmed1975@ukm.edu.my

an efficient and encouraging approach with many benefits of no specific material needed, non-expensive and simple technique [23]. Several inhibitors have been discovered in the past decade.

Organic molecules with electronegative negative atoms, including phosphorous, sulfur, oxygen, and nitrogen, and molecules containing pi bonds in their molecular structures are effective corrosive inhibitor compounds [24-27]. Organic molecules exhibit corrosion-inhibitory characteristics during physisorption and/or chemisorption. This property is attributed to their active sites interacting with metallic surfaces [28-30]. Since the thiosemicarbazones and thiosemicarbazide are significant, We synthesized phenylthiosemicarbazide with the benzaldehyde moiety. Its anti-corrosion behaviors towards the corrosions of the MS in 1 M HCl were researched. This molecule has been selected to examine its anti-corrosion efficacy due to the aromatic ring, benzaldehyde nucleus, and nitrogen atoms. These atoms were facilitated adsorption on MS surfaces. Therefore, these structures make the adsorption easier on an MS surface. In addition, a vacant d-orbital of the sulfur atom in the thiosemicarbazide exists. This event results in the likelihood of the formation of the dπ−dπ bond with the 3-D electrons of the iron. Considering to clean environment and green chemistry, (3-nitrobenzaldehyde)-4-phenylthiosemicarbazone (3N-4P) has been synthesized by a traditional approach, and ethanol used as a solvent. Then, its effects of corrosion inhibition compared to the MS corrosions in the acidic mediums were assessed.

2. Experimental

2.1. Material and sample preparation

Solvents and other analytical grade chemicals were purchased from Sigma-Aldrich and synthesized the targeted inhibitor without further purification. MS samples with a composition of Carbon: 0.210 %, Silicone: 0.380 %, Aluminum 0.010 %, Manganese: 0.050 %, Sulfur: 0.050 %, Phosphorous: 0.090 % and iron is used for the remaining elements. The steel samples were polished and cleaned with distilled water and finally immersed in acetone and dried.

2.2. Characterization techniques

FT-IR spectrum was carried out utilizing a Nicolet 6700 FT-IR spectrophotometer (Thermo Nicolet Corp., Madison, WI, USA) in the 4000–400 cm^{-1} region using KBr pellets for confirmation and identification of different functional groups present in the synthesized inhibitor. Proton nuclear magnetic resonance (^{1}H-NMR) and Carbon-13 nuclear magnetic resonance (^{13}C-NMR) spectra were reported on a spectrometer instrument with 600 MHz (Bruker, Billerica, MA, USA), at room temperature in DMSO-d6, utilizing Tetramethylsilane (TMS) as the internal standard. Tetramethylsilane is the accepted internal standard for calibrating chemical shifts for NMR spectroscopy. ^{1}H-NMR is the employment of nuclear magnetic resonance in NMR spectroscopical technique concerning hydrogen-1 nuclei within the organic molecule to confirm the structure of its molecule. ^{13}C-NMR utilizes nuclear magnetic resonance (NMR) spectroscopical technique to carbon and identifies carbon atoms in organic molecules.

2.3. Synthesis (3-nitrobenzaldehyde)-4-phenyl-thiosemicarbazone (3N-4P), as a corrosion inhibitor

The target inhibitor (3N-4P) was synthesized by the reaction of 3-nitrobenzaldehyde (0.002 mmol) and 4-phenylthiosemicarbazide (0.002 mmol) in ethyl alcohol (100 mL). The reaction mixture was refluxed for 10 h. Thin-layer chromatography (TLC) was used to examine the purity of the final compound (3N-4P), which was then filtered, washed with alcohol, and dried. Yield 49 %, M.P. 204-206 °C. FTIR, ^{1}H-NMR, and ^{13}C-NMR spectroscopy, as well as CHN elemental analysis, was used to describe and confirm the chemical structure of the yellow product. FTIR (cm^{-1}): 3245.36 and 3219.85 for N–H, 1644.62 for C=N, and 1542.14 for C-H aromatic. ^{1}HNMR, DMSO-d^{6}, δ: 8.32 ppm (1H, d, NH); 7.27-8.11 ppm (1H, m, $CH_{aromatic}$); and 8.16-8.29 ppm (1H, m, $CH_{aromatic}$). ^{13}CNMR, DMSO-d^{6}, δ: 122.68,126.3, 126.9, 127.1, 127.9, 128.3, 129.6, 133.1, 135.8, 140.3, 146.8 and 149.3, 177.9. The elemental analysis (Found/Calculated): C, 56.38/55.99; H, 4.11/4.03; N, 18.93/18.65.

2.4. Weight loss techniques

The steel samples were exposed to an environment of 1.0 M hydrochloric acid with varying concentrations (1 to 5 mM) of the 3N-4P as corrosion inhibitor for 10 h in a water bath at a 303 K. The tested steel samples were taken and washed with double distilled with water then acetone. Each experiment was repeated three-time,

and an average was used. The same approach was conducted for various temperatures (303, 313, 323, and 333 K) and concentrations of the 3N-4P.

2.5. Scanning electron microscopy (SEM)

An SEM was utilized to investigate the surface of MS coupons (scanning electron microscopy, Tabletop Microscope/TM1000 Hitachi). The coupons were immersed in a corrosive solution with and without 3N-4P for 5 h.

3. Results and Discussion

3.1. Synthesis of the 3N-4P

As depicted in Figure 1, the reaction scheme was followed to synthesize 3N-4P. The target was created by dehydration reaction of phenylthiosemicarbazide with 3-nitrobenzaldehyde under reflux and using ethanol as a solvent. The structure of 3N-4P was confirmed by spectroscopically methods (FTIR and NMR) and CHN analysis.

3.2. Weight loss techniques: Effect of 3N-4P concentration.

The rate of corrosion (C_R) and protection efficacy (IE %) of the 3N-4P at different concentrations (1 mM to 5 mM) and temperatures (303 to 333 K) for (1, 5, 10, 24, and 48 h) as immersion time, were evaluated by weight loss techniques, as the experimental findings are postulated in Figures 2 and 3. The rate of corrosion (C_R) and inhibitory efficiency (IE%) were determined based on equations 1 and 2.

$$C_R = \frac{\Delta W}{St} \quad (1)$$

$$IE(\%) = \frac{C_{Ra} - C_{RP}}{C_{Ra}} \times 100 \quad (2)$$

Where ΔW refers to the loss of weight, S represents the immersed area, t is the exposure period and C_{Ra}, and C_{Rp} are the corrosion rates without and with 3N-4P, respectively.

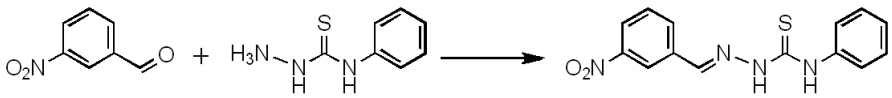

Figure 1: Schematic route of 3N-4P.

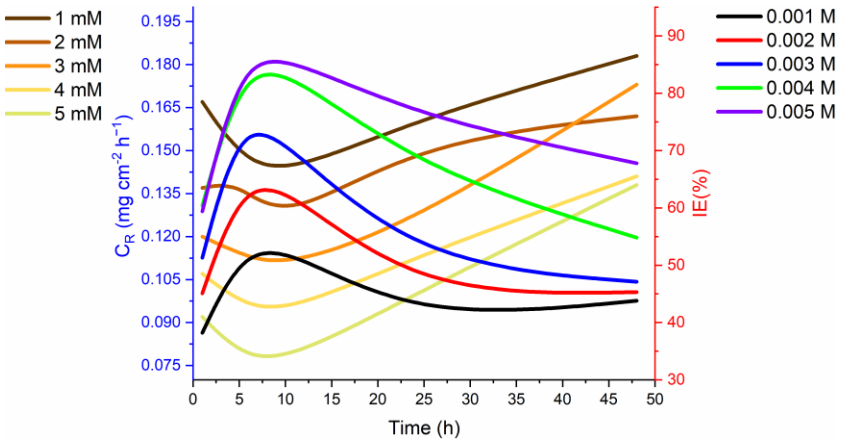

Figure 2: Experimental findings of weight loss techniques of MS after (1, 5, 10, 24, and 48 h) immersion in 1 M HCl with the addition of various concentrations (1, 2, 3, 4, and 5 mM) of the 3N-4P at 303 K.

The inhibition efficacy improved on increasing the 3N-4P concentration, and a reduction in the C_R was found at all studied concentrations (i.e., 1-5 mM), as seen in Figure 2. Thus, it is clear that the inhibition efficacy was dependent on the studied inhibitor concentration. More molecules of 3N-4P are adsorbed on the MS coupon at increasing concentration of the studied inhibitor resulting in an improvement in the inhibition quality. The molecules which have been adsorbed block the reaction sites and protect the coupon surface from corrosion. As free electrons are available on the azomethine (imine) and also a pair of electrons on S and N atoms in addition to pi-electrons will be closely bound to the MS surface, corrosion might be hindered. From Figure 2, it is clear that the C_R of immersed coupon in corrosive solution is found to reduce with increasing immersion period (until 10 h) and 3N-4P concentration. These findings could be due to the increase in the number of the molecules of the tested inhibitor adsorbed on the coupon surface, which isolates the coupon surface from the hydrochloric acid solution, conducting impediment of coupon dissolution. After 10 h of immersion period, the inhibitive performance was reduced. [31, 32]. The diminished inhibition activity was due to the desorption of the inhibitor molecules onto the coupon surface.

Moreover, the C_R was increased with the exposure period increase. This result can be demonstrated regarding the theory of adsorption. When 3N-4P molecules onto the coupon surface were desorbed, a coupon was exposed to a corrosive environment, thereby increasing the contact of a coupon surface/HCl solution, which results in the dissolution of MS. Moreover, the C_R increases with the immersion period increasing due to a low molecule number of 3N-4P in an acidic solution to impedance the coupon dissolution. Visual examination of the absence and presence of the tested corrosion inhibitor demonstrated that the tested coupon almost maintained its light exterior with the addition of inhibitor, while those exposed to the HCl solution without the inhibitor did not. This result supported that this inhibitor was significantly active in preventing corrosion attacks and the C_R [33, 34].

3.3. Weight loss measurements: effect of temperature.

Temperature considerably determines the corrosion rate (C_R), and with temperature increasing, the C_R increases extensively in the hydrochloric acid solution. The weight loss was calculated between 303 and 333 K to consider the inhibition efficacy of the synthesized inhibitor at higher temperatures. The highest IE% was seen of the synthesized inhibitor at 303 K, which reduced gradually with further temperature increases.

From Figure 3, it is evident that at the higher temperature, the analyzed inhibitor displayed lower efficiency because higher temperature degrees did not promote fundamental forces (physical interactions) and hence decreased the inhibitory effect. At higher temperature degrees, adsorption and desorption begins after a brief period and expose the metal surface to the surrounding acidic environment for a longer time, decreasing the influence of inhibition.

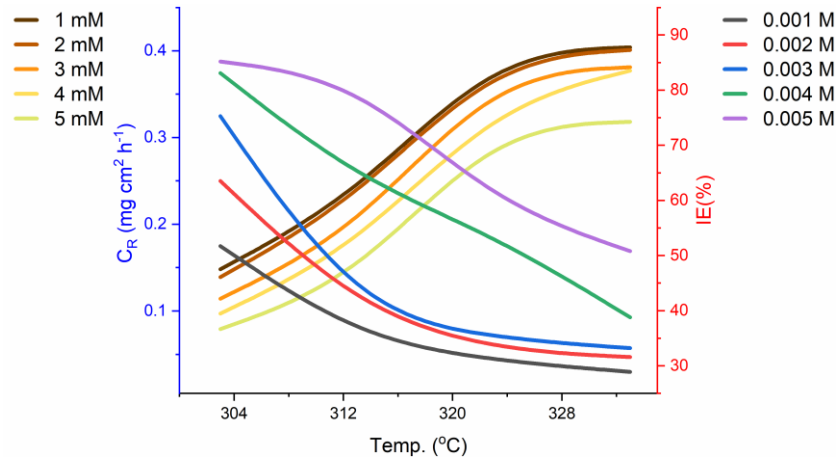

Figure 3: Experimental findings of weight loss measurements of MS after five h immersion in 1 M hydrochloric acid with various 3N-4P concentrations (1, 2, 3, 4, and 5 mM) at different temperatures (303 to 333 K).

Arrhenius equation gives the relationship between the temperature and the C_R as in equation 3:

$$C_R = K \exp\left[-\frac{E_a^*}{RT}\right] \quad (3)$$

where, E_a^* is the activation energy, k is the Arrhenius parameter, R is the gas constant, and T is the temperature

Arrhenius equation alternative as in equation 4

$$C_R = \frac{RT}{Nh} \exp\left[\frac{\Delta S_a^*}{R}\right] \exp\left[-\frac{\Delta H_a^*}{RT}\right] \quad (4)$$

Where ΔH_a^* is the enthalpy, ΔS_a^* is the entropy, N is the number of Avogadro and h is the constant of Planck.

The activation energy and k value for tested MS at various concentrations in absence and presence inhibitor was evaluated from the intercept and slope values of the Arrhenius plot between log C_R and the value of 1/T, as shown in Figure 4. The enthalpy was calculated from the slope, which is represented by $-\Delta H_a^*/R$. On the other hand, the entropy was calculated from intercept value which is represented by $\ln(R/Nh) + \Delta S_a^*/R$ of the plot between $\log C_R/T$ and $1/T$ as in Figure 5.

The reduction in the inhibition performance with increasing temperature was due to the activation energy of the studied inhibitor solution being higher than that of the blank solution. The experimental findings of this test justify the assertion that activation energy rises with an increase in temperature because of the decrease in physical adsorption. The activation energy measurements showed that the value activation energy was higher with the addition of 3N-4P relative to that without 3N-4P, which was 39.58 kJ mol^{-1} (Table 1). The increased activation energy value is related to the formation of 3N-4P molecules-Fe complex in the hydrochloric acid solution with a considerable energy barrier [35-37]. The positive value of enthalpy in the addition of the tested inhibitor proposed the endothermic dissolution of metal.

3.4. Adsorption isotherms

The interaction between the 3N-4P molecules and coupon surface was better investigated using chemisorption or physisorption-based adsorption isotherms. The surface coverage degree of the 3N-4P is mainly affected by the C_R. The IE% is therefore referred to as the function of the electrode surface covered by a degree molecule [38, 39]. The concentration and surface coverage degree utilized in determining the linear relationship of adsorption isotherm. The surface coverage (θ) was determined based on equation 5.

$$\theta = \left[\frac{IE}{100}\right] \quad (5)$$

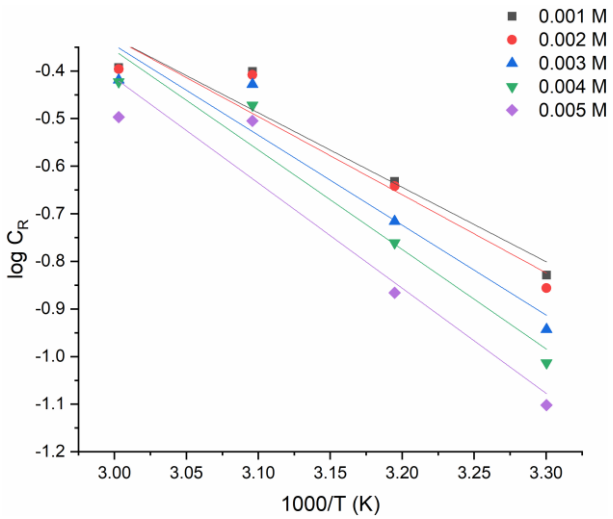

Figure 4: Arrhenius plot for MS in 1 M HCl with various concentrations (1, 2, 3, 4, and 5 mM) of 3N-4P.

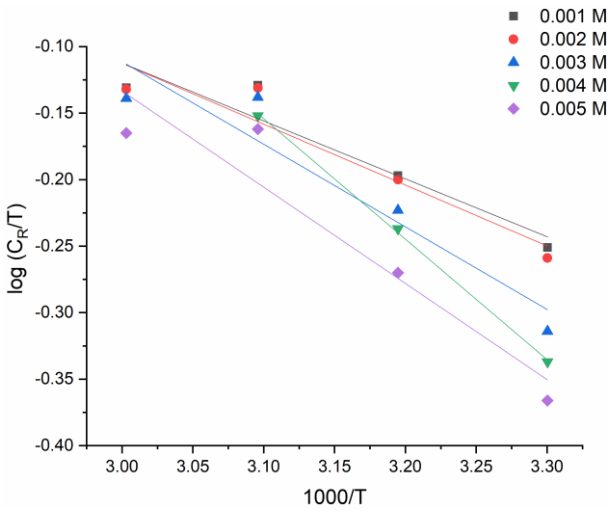

Figure 5: Arrhenius plot alternative for MS in 1 M HCl with various concentrations (1, 2, 3, 4, and 5 mM) of 3N-4P.

Different adsorption models, including Langmuir, Temkin, and Frumkin, were tested to understand the inhibition mechanism, and the model of Langmuir model was fitted. The relation between surface coverage and concentration can be determined according to equation 6, where K_{ads} is the equilibrium constant.

$$\frac{C}{\theta} = \frac{1}{K_{ads}} + C \quad (6)$$

Figure 6 represents the relationship between C and C/θ. The linear relation suggests that the 3N-4P molecules adsorbed on the MS surface obeyed the Langmuir model.

To calculate the adsorption free energy ΔG^{o}_{ads} and K_{ads} was calculated according to equation 7, where 55.5 ($mol.dm^{-3}$) is water concentration.

$$\Delta G^{o}_{ads} = -RT\ln(55.5K_{ads}) \quad (7)$$

The ΔG^{o}_{ads} was −38.21 $kJ.mol^{-1}$ (Table 1), suggesting that 3N-4P molecules adsorbed on the MS surface were spontaneous. According to the report, free energy values around −20 kJ mol^{-1} indicate physisorption interactions. In contrast, those around −40 $kJ.mol^{-1}$ refer to chemisorption interactions. Herein, the free energy value was −38.21 kJ mol^{-1}, which marked physisorption and chemisorption [40].

3.5. Suggested mechanism

By using weight loss techniques, the inhibition mechanism of MS with 3N-4P in the acid solution has been characterized through adsorption of the corrosion product. Generally, the corrosion inhibitory results in the mitigation of corrosion in one of those ways: (a) Inhibitive results of the reduction of the C_R were due to the adsorbed 3N-4P molecules on the MS surface. (b) It can form a base metal oxide film, (c) It can also react with the corrosive component that exists in the corrosive medium and results in a complex. The 3N-4P molecules which be adsorbed over the surface of the metal; as a result, they reduce the C_R. It has been well accepted that corrosion inhibitor adsorption is a competitive phenomenon that replaces the water molecules that are adsorbed already on the coupon surface and as a result of the adsorbed itself based on equation (5). The inhibitor molecule adsorption on MS surfaces can happen in several approaches: (a) can adsorb electro-statically on the surface of the metal. (b) can adsorb by donating the unshared pair of electrons located on the aromatic system π-electrons or heteroatoms to the vacant 3-d iron orbital. (c) the retro donation can also result in the adsorptions of the molecule of the 3N-4P on the MS coupon. A study of the 3N-4P structure has shown that the existence of the isotherm has facilitated physical interactions, but the unshared pairs of the electron, which reside on π-electrons and heteroatom, result in chemical interactions with the coupon surface. Similar results have been stated earlier by different researchers. 3N-4P is better than benzaldehyde and furfuraldehyde hydrazones,

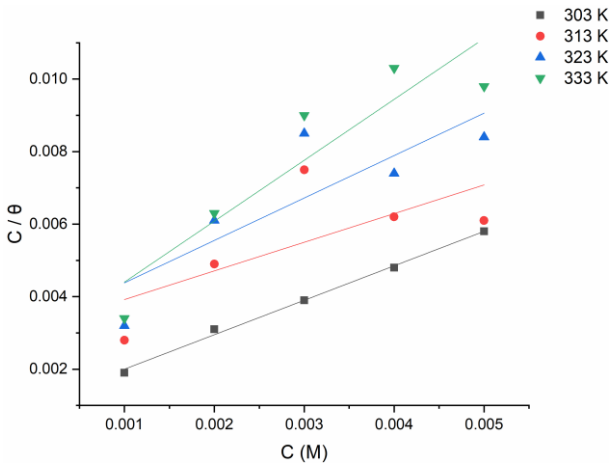

Figure 6: Langmuir isotherm for the 3N-4P on MS in 1 M corrosive environment at various Temperatures.

Table 1: Thermodynamically parameters were obtained from mass loss of mild steel in 1 M HCl containing five mM of tested inhibitor at 303 K.

C_R	IE%	E^*_a	ΔS^*_a	ΔH^*_a	ΔG^o_{ads}	θ
0.08	85.7	39.58 kJ mol^{-1}	98.37 $Jmol^{-1}.K^{-1}$	57.75 kJ mol^{-1}	−38.21 kJ mol^{-1}	0.85

which were previously researched. The likelihood of dπ−dπ bonding between the 3-d electrons of the atom of iron and vacant S atom $3_{d\text{-orbital}}$ of the thiosemicarbazone nucleus results in appreciable 3N-4P efficiency at greater concentration levels even at greater temperatures [41, 42]. Those inhibitor types offer d-electrons and have vacant d-orbitals to accept the metal electrons that form stable chelates that were researched already as excellent inhibitors [43, 44]. The proposed mechanism model of adsorption of 3N-4P on the coupon surface in hydrochloric acid solution was postulated in Figure 7.

3.6. Surface study

SEM studies of the 3N-4P particles on coupon surface were conducted without and with five mM of 3N-4P in 1 M HCl to determine the adsorption process. Figure 8a represents the coupon surface without adding inhibitor, and it is evident that the coupon surface is corroded strongly. From Figure 8b, it is obvious that the coupon surface is smooth and uncorroded, indicating that the studied inhibitor demonstrated a high impedance corrosion degree in acid solution at 303 K.

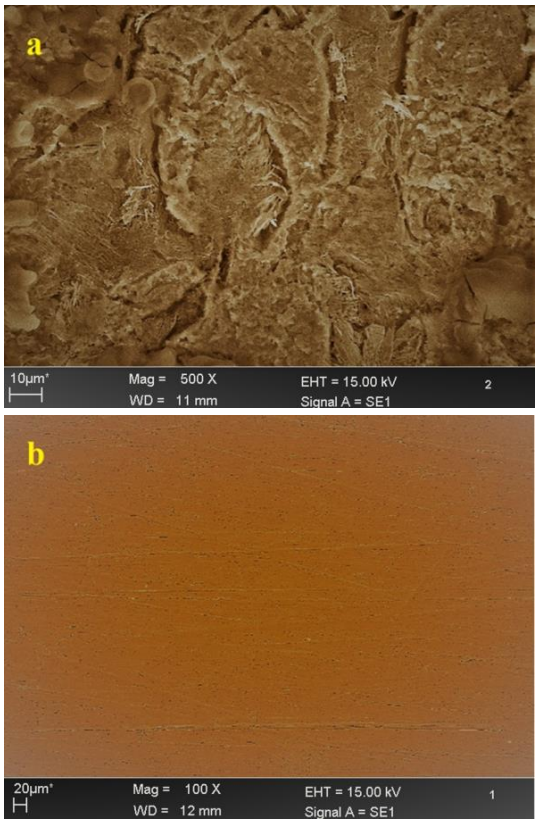

Figure 8: a) Represents the coupon surface without adding 3N-4P and (b) with 3N-4P.

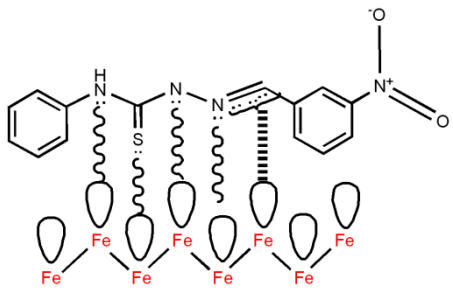

Figure 7: The postulated mechanism of 3N-4P molecules on coupon surface in 1 M HCl environment.

4. Conclusion

In brief, we showed the synthesis of a new Schiff base, namely "(3-nitrobenzaldehyde)-4-phenylthiosemicarbazone (3N-4P)" and explored its ability to serve as a corrosion inhibitor. The studied molecules demonstrated significant inhibitive performance for steel in 1 M HCl. The weight-loss study found that the protection efficacy improved with the increase in the inhibitor concentration and reduced with a temperature rise. The analysis of adsorption isotherms showed physisorption, and the isotherm was the Langmuir form. In comparison, the SEM photos show a protective coating on the coupon that controls and inhibits the corrosion.

5. References

1. A. Al-Amiery, L. Shaker, A. Kadhum, M. Takriff, Corrosion inhibition of mild steel in strong acid environment by 4-((5,5-dimethyl-3-oxocyclohex-1-en-1-yl)amino)benzenesulfonamide. *Tribol. Indust.*, 42(2020), 89-101.
2. K. Aly, A. Mahdy, M. Hegazy, N. Al-Muaikel, S. Kuo, M. Gamal Mohamed, Corrosion resistance of mild steel coated with phthalimide-functionalized polybenzoxazines, *Coatings*, 10(2020), 1114.
3. A. Al-Amiery, T. Salman, K. Alazawi, L. Shaker, A. Kadhum, M. Takriff, Quantum chemical elucidation on corrosion inhibition efficiency of Schiff base: DFT investigations supported by weight loss and SEM

techniques. *Inter. J. Low-Carbon Technol.*, *15*(2020), 202–209.
4. A. Al-Amiery, L. Shaker, A. Kadhum, M. Takriff, Synthesis, characterization and gravimetric studies of novel triazole-based compound, *Inter. J. Low-Carbon Technol.*, *15* (2020), 164–170.
5. K. Aly, M. Mohamed, O. Younis, M. Mahross, M. Abdel-Hakim, M. Sayed, Salicylaldehyde azine-functionalized polybenzoxazine: Synthesis, characterization, and its nanocomposites as coatings for inhibiting the mild steel corrosion, *Prog. Org. Coat.*, 138(2020), 105385.
6. K. Aly, O. Younis, M. Mahross, E. Orabi, M. Abdel-Hakim, O. Tsutsumi, M. Sayed, Conducting copolymers nanocomposite coatings with aggregation-controlled luminescence and efficient corrosion inhibition properties, *Prog. Org. Coat.*, 135(2019), 525-535.
7. A. Al-Amiery, A. Kadhum, A. Kadihum, A., Mohamad, C. How, S. Junaedi, Inhibition of mild steel corrosion in sulfuric acid solution by new schiff base, *Mater.*, *7*(2014), 787–804.
8. A. Al-Amiery, L. Shaker, Corrosion inhibition of mild steel using novel pyridine derivative in 1 M hydrochloric acid. *Koroze Ochr. Mater.*, *64*(2020), 59-64. 9
9. A. Al-Amiery, Anti-corrosion performance of 2-isonicotinoyl-n-phenylhydrazinecarbothioamide for mild steel hydrochloric acid solution: Insights from experimental measurements and quantum chemical calculations, *Surf. Rev. Lett.*, 28(2021), 1-8.
10. M. Mohamed, S. Kuo, A. Mahdy, I. Ghayd, K. Aly, Bisbenzylidene cyclopentanone and cyclohexanone-functionalized polybenzoxazine nanocomposites: Synthesis, characterization, and use for corrosion protection on mild steel, *Mater. Today Commun.*, 25(2021), 101418.
11. M. Mohamed, A. Mahdy, R. Obaid, M. Hegazy, S. Kuo, K. Aly, Synthesis and characterization of polybenzoxazine/clay hybrid nanocomposites for UV light shielding and anti-corrosion coatings on mild steel, *J. Poly. Res.*, 28(2021), 297.
12. S. Al-Baghdadi, T. Gaaz, A. Al-Adili, A., Al-Amiery, M. Takriff, Experimental studies on corrosion inhibition performance of acetylthiophene thiosemicarbazone for mild steel in HCl complemented with DFT investigation, *Inter. J. Low-Carbon Technol.*, 16(2021), 181-188.
13. S. Al-Baghdadi, F. Hashim, A. Salam, T. Abed, T. Gaaz, A. Al-Amiery, A. Kadhum, K. Reda, W. Ahmed, Synthesis and corrosion inhibition application of NATN on mild steel surface in acidic media complemented with DFT studies, *Res. Phy.*, 8(2018), 1178-1184.
14. S. Al-Baghdadi, A. Al-Amiery, A. Kadhum, M. Takriff, Computational Calculations, Gravimetrical, and surface morphological investigations of corrosion inhibition effect of triazole derivative on mild steel in HCl, *J. Comp. Theoret. Nanosci.*, 17(2020), 4797-4804.
15. S. Al-Baghdadi, A. Kadhim, G. Sulaiman, A. Al-Amiery, A. Kadhum, M. Takriff, Anticorrosion and antibacterial effects of new Schiff base derived from hydrazine, *J. Phys.: Conf. Series*, 1795(2021), 012021. 1
16. S. Al-Taweel, T. Gaaz, L. Shaker, A. Al-Amiery, Protection of mild steel in h2so4 solution with 3-((3-(2-hydroxyphenyl)-5-thioxo-1,2,4-triazol-4-yl)imino)indolin-2-one, *Inter. J. Corrosion Scale Inhib.*, 9(2020), 1014-1024.
17. A. Alamiery, E. Mahmoudi, T. Allami, Corrosion inhibition of low-carbon steel in hydrochloric acid environment using a Schiff base derived from pyrrole : gravimetric and computational studies, *Inter. J. Corrosion Scale Inhib.*, 1*0*(2021), 749-765.
18. A. Alamiery, L. Shaker, T. Allami, A. Kadhum, S. Takriff, A study of acidic corrosion behavior of Furan-Derived schiff base for mild steel in hydrochloric acid environment: Experimental, and surface investigation. *Materials Today: Proceedings*, *44* (2021), 2337–2341.
19. A. Eltmimi, A. Alamiery, T. Allami, M. Yusop, Inhibitive effects of a novel efficient Schiff base on mild steel in hydrochloric acid environment, *Inter. J. Corros. Scale Inhib.*, 4(2021), 634-648.
20. H. Habeeb, H. Luaibi, T. Abdullah, R. Dakhil, A. Kadhum, A. Al-Amiery, Case study on thermal impact of novel corrosion inhibitor on mild steel, *Case Studies Thermal Eng.*, 12(2018), 64-68. h
21. H. Habeeb, H. Luaibi, R. Dakhil, A. Kadhum, A. Al-Amiery, T. Gaaz,. Development of new corrosion inhibitor tested on mild steel supported by electrochemical study, *Results Phys.*, 8(2018), 1260-1267.
22. M. Hanoon, A. Resen, L. Shaker, A. Kadhum, A. Al-Amiery, Corrosion investigation of mild steel in aqueous hydrochloric acid environment using n-(Naphthalen-1yl)-1-(4-pyridinyl)methanimine complemented with antibacterial studies, *Biointerface Res. Appl. Chem.*, 11(2021), 9735-9743.
23. M. Hanoon, D. Zinad, A. Resen, A. Al-Amiery, Gravimetrical and surface morphology studies of corrosion inhibition effects of a 4-aminoantipyrine derivative on mild steel in a corrosive solution, *Inter. J. Corrosion Scale Inhib.*, 9(2020), 953-966.
24. D. Jamil, A. Al-Okbi, S. Al-Baghdadi, A. Al-Amiery, A. Kadhim, T. Gaaz, A. Kadhum, A. Mohamad, Experimental and theoretical studies of Schiff bases as corrosion inhibitors, *Chem. Central J.*, 12(2018), 77-82.
25. Q. Jawad, A. Hameed, M. Abood, A. Al-Amiery, L. Shaker, A. Kadhum, M. Takriff, Synthesis and comparative study of novel triazole derived as corrosion inhibitor of mild steel in hcl medium complemented with dft calculations, *Inter. J. Corrosion Scale Inhib.*, 9(2020), 688-705.

26. S. Junaedi, A. Al-Amiery, A. Kadihum, A. Kadhum, A. Mohamad, Inhibition effects of a synthesized novel 4-aminoantipyrine derivative on the corrosion of mild steel in hydrochloric acid solution together with quantum chemical studies, *Inter. J. Mol. Sci.*, 14(2013), 11915-11928.
27. S. Junaedi, A. Kadhum, A. Al-Amiery, A. Mohamad, M. Takriff, Synthesis and characterization of novel corrosion inhibitor derived from oleic acid: 2-Amino 5-Oleyl-1,3,4-Thiadiazol (AOT), *Inter. J.Electrochem. Sci.*, 7(2012), 3543-3554.
28. S. Junaedi, A. Al-Amiery, A. Kadihum, A. Kadhum, A. Mohamad, Inhibition effects of a synthesized novel 4-aminoantipyrine derivative on the corrosion of mild steel in hydrochloric acid solution together with quantum chemical studies, *Inter. J. Mol. Sci.*, 14(2013), 11915-11928.
29. A. Kadhim, A. Al-Amiery, R. Alazawi, M. Al-Ghezi, R. Abass, Corrosion inhibitors. A review, *Inter. J. Corrosion Scale Inhib.*, 10(2021), 54-67.
30. A. Kadhim, A. Al-Okbi, D. Jamil, A. Qussay, A. Al-Amiery, T. Gaaz, A. Kadhum, A. Mohamad, M. Nassir, Experimental and theoretical studies of benzoxazines corrosion inhibitors, *Results Phys.*, 7*(*2017), 4013-4019.
31. A. Kadhim, G. Sulaiman, A. Abdel Moneim, R. Yusop, A. Al-Amiery, Synthesis and characterization of triazol derivative as new corrosion inhibitor for mild steel in 1M HCl solution complemented with antibacterial studies, *J. Phys.: Conference Series*, 1795(2021), 012011.
32. A. A. H. Kadhum, A. B. Mohamad, H. D. Jaffar, S. S. Yan, J. H. Naama, A. A. Al-Tamimi, R. I. Al-Bayati, A. A. Al-Amiery, Corrosion of nickel-aluminum-bronze alloy in aerated 0.1 M sodium chloride solutions under hydrodynamic condition, *Inter. J. Electrochem. Sci.*, 8(2013), 37-46.
33. H. Obayes, A. Al-Amiery, G. Alwan, T. Abdullah, A. Kadhum, A. Mohamad, Sulphonamides as corrosion inhibitor: Experimental and DFT studies, *J. Mol. Struct.*, 1138(2017), 1-9.
34. A. Resen, M. Hanoon, W. Alani, A. Kadhim, A., Mohammed, T. Gaaz, A. Kadhum, A. Al-Amiery, M. Takriff, Exploration of 8-piperazine-1-ylmethylumbelliferone for application as a corrosion inhibitor for mild steel in hydrochloric acid solution, *Inter. J. Corrosion Scale Inhib.*, 10(2021), 368-387.
35. A. Salim, Q. Jawad, K. Ridah, L. Shaker, A. Al-Amiery, A. Kadhum, M. Takriff, Corrosion inhibition of thiadiazole derivative for mild steel in hydrochloric acid solution, *Inter. J. Corrosion Scale Inhib.*, 9(2020), 550-561.
36. A. Salman, Q. Jawad, K. Ridah, L. Shaker, A. Al-Amiery, Selected BIS-thiadiazole: synthesis and corrosion inhibition studies on mild steel in HCl environment, *Surf. Rev. Lett.*, 27(2020), 1-5.
37. T. Salman, Q. Jawad, M. Hussain, A. Al-Amiery, L. Mohamed, A. Kadhum, M. Takriff, Novel ecofriendly corrosion inhibition of mild steel in strong acid environment: Adsorption studies and thermal effects, *Inter. J. Corrosion Scale Inhib.*, 8(2019), 1123-1137.
38. T. Salman, Q. Jawad, M. Hussain, A. Al-Amiery, L. Shaker, A. Kadhum, M. Takriff, New environmental friendly corrosion inhibitor of mild steel in hydrochloric acid solution: Adsorption and thermal studies, *Cogent Eng.*, 7(2020), 1826077.
39. L. Shaker, A. Al-Adili, A. Al-Amiery, M. Takriff, The inhibition of mild steel corrosion in 0.5 M H_2SO_4 solution by N-phenethylhydrazinecarbothioamide (N-PHC), *J. Phys.: Conference Series*, 1795(2021), 012009.
40. E. Sheet, J. Yamin, H. Al-Salihi, A. Salam, K. Reda, W. Ahmed, M. Mahdi, A. Al-Amiery, N-(3-nitrobenzylidene)-2-aminobenzothiazole as new locally available corrosion inhibitor for iraqi oil industry, *J. Balkan Tribol Assoc*, 26(2020), 194-203.
41. J. Yamin, E. Sheet, A. Al-Amiery, Statistical analysis and optimization of the corrosion inhibition efficiency of a locally made corrosion inhibitor under different operating variables using RSM, *Inter. J. Corrosion Scale Inhib.*, 9(2020), 502-518.
42. D. Zinad, M. Hanoon, R. Salim, S. Ibrahim, A. Al-Amiery, M. Takriff, A. Kadhum, A new synthesized coumarin-derived schiff base as a corrosion inhibitor of mild steel surface in hcl medium: Gravimetric and dft studies, *Inter. J. Corrosion . Scale Inhib.*, 9(2020), 228-243.
43. D. Zinad, Q. Jawad, M. Hussain, M. Mahal, L. Mohamed, A. Al-Amiery, Adsorption, temperature and corrosion inhibition studies of a coumarin derivatives corrosion inhibitor for mild steel in acidic medium: Gravimetric and theoretical investigations, *Inter. J. Corrosion Scale Inhib.*, 9(2020), 134-151.
44. D. Zinad, A. Mahal, A. Al-Amiery, An Efficient Synthesis of Novel Imidazo-Aminopyridinyl Derivatives from 2-Chloro-4-cyanopyridine, *Org. Prepar. Proced. Internat.*, 52(2020), 361-367.

How to cite this article:
A. M. Mustafa, Z. S. Abdullahe, F. F. Sayyid, M. M. Hanoon, A. A. Alamiery, W.N.R.W. Isahak, 3-Nitrobenzaldehyde-4-Phenylthiosemicarbazone as Active Corrosion Inhibitor for Mild Steel in a Hydrochloric Acid Environment. Prog. Color Colorants Coat., 15 (2022), 285-293.